JOURNAL OF MATERIALS SCIENCE 29 (1994) 1056–1066

Pulse chemical vapour deposition and infiltration of pyrocarbon in model pores with rectangular cross-sections

Part II *Study of the infiltration*

P. DUPEL, R. PAILLER, X. BOURRAT, R. NASLAIN
Laboratoire des Composites Thermostructuraux UMR 47 CNRS-SEP-UB1, Domaine Universitaire, 3 allée de La Boëtie, 33600 Pessac, France

Model straight pores with rectangular cross-section (size ranging from 60 to 320 μm) have been infiltrated with pyrocarbon resulting from the cracking of C_3H_8 or CH_4 under pulse chemical vapour infiltration (P-CVI) conditions. Three main parameters control the quality of the pore infiltration: temperature and pressure, as previously known for regular CVI under isothermal/isobaric conditions (I-CVI) and, additionally, the residence time t_R, which appears to be the key parameter in P-CVI. There is a direct correlation between t_R, on the one hand, and both the PyC thickness gradient and anisotropy along the pores, on the other hand. The experimental results are explained on the basis of a qualitative model assuming two competing deposition mechanisms, depending on whether PyC is formed from small and H-rich molecules (akin to C_3H_8) (low t_R values) or from large aromatic H-poor intermediates resulting from the maturation of the gas phase (high t_R values). The use of CH_4 (more stable thermally than C_3H_8) slows down the maturation process and favours in-depth infiltration. The best infiltrations, similar to and even better than those reported for I-CVI, are achieved under low t_R, T, P conditions but require a very large number of pulses. P-CVI is an efficient way to control the microstructure of the deposit.

1. Introduction

Chemical vapour infiltraton (CVI), when performed under isothermal/isobaric conditions (I-CVI), has been shown to be a processing technique well suited to the fabrication of ceramic matrix composites (CMC), particularly when the matrix is a non-oxide material (e.g. carbon, carbides, nitrides) [1–5]. One of its important advantages, from a practical point of view, is its ability to be used for the simultaneous treatment of a large number of fibre preforms even of different sizes and shapes. Conversely I-CVI is known to exhibit some drawbacks: (i) it requires relatively long processing times and some crust removal and (ii) it yields CMC with a residual porosity of 10–15%.

Attempts have been made to reduce the processing time by applying to the fibre preform pressure/temperature gradients, replacing thus the slow diffusion mass transfer in the pore network by forced-convection mass transfer and increasing the in-depth deposition rate of the matrix by an increase of the temperature. However, this forced CVI (F-CVI) exhibits strong limitations on preform tooling, on the one hand, and the size and number of preforms, on the other hand [3, 6].

Another attractive alternative could be the use of pulse CVI (P-CVI) in which the porous fibre preform is submitted, at a high frequency, to cycles comprising: (i) the injection of the feed gas in the preform by forced convection in a very short time, (ii) holding the feed gas in the preform during a time long enough to permit the deposition of the matrix with a high growth rate but short enough to avoid the poisoning effect of the reaction gaseous products, and (iii) evacuating the residual gas phase [7–10]. P-CVI is expected to exhibit the following advantages: (i) it may reduce (and even suppress) the deposit density gradient in the preform and (ii) it may yield high deposition rates, while keeping the main advantage of I-CVI, i.e. its suitability for the simultaneous treatment of a large number of different preforms. Conversely, P-CVI introduces new constraints such as the difficulty related to the filling and evacuation of large furnaces in very short times.

Generally speaking, P-CVI and particularly that of pyrocarbon has not been extensively studied yet from either an experimental or a theoretical point of view, and its suitability for the processing of CMC has still to be established. The aim of the present contribution, which is the second part of a series of articles devoted to P-CVD/P-CVI [11, 12], was to demonstrate experimentally the interest and limitations of this new processing technique, focusing on the one hand, on pyrocarbon and model pore infiltration, and on the other hand on the influence of various parameters (temperature, pressure, residence time, precursor nature, pore aspect ratio) on the infiltration efficiency.

0022–2461

2. Experimental procedure

The P-CVD/P-CVI experiments were performed with the apparatus and procedure described in Part I [11]. It will be sufficient to recall here that: (i) pyrocarbon (PyC) is deposited (or infiltrated) as the result of the cracking of a hydrocarbon (the precursor) which is either propane (C_3H_8) or methane (CH_4), the former being more reactive than the latter, under the following conditions: $900 < T < 1150\,°C$; $1 < P < 1000$ kPa; $0.5 < t_R < 100$ s, t_R being the residence time of the gas in the furnace, and (ii) the substrate consists of a block of purified graphite made of two bolted parts with three straight pores of rectangular cross-sections at the interface. The pores have the same length ($L = 20$ mm) and their cross-sections are characterized by the same width ($l = 2$ mm) but exhibit different heights (namely 60, 120 and 320 μm).

After each deposition/infiltration experiment, the two part graphite block is unbolted and the grooved half-part cut with a diamond saw along each of the model pore axes. The longitudinal sections are then polished with diamond pastes of decreasing grain sizes (down to 1 μm) and observed with an optical microscope (MeF_3 from Reichert-Jung). Two kinds of measurement were systematically performed for each longitudinal section: (i) the thickness of the PyC deposit along the z-axis of the pore (the origin of the z-coordinate being the pore entrance), and (ii) the extinction angle Ae used as a representative parameter of the anisotropy of the PyC microstructure, as discussed in more detail elsewhere [12].

The quality of the pore infiltration will be characterized in the following by the thickness profile along the pore longitudinal z-axis and by the degree of filling of the pore, referred to as the filling ratio δ_i, calculated by integrating the thickness profile along the pore length and dividing the result by half of the initial pore volume.

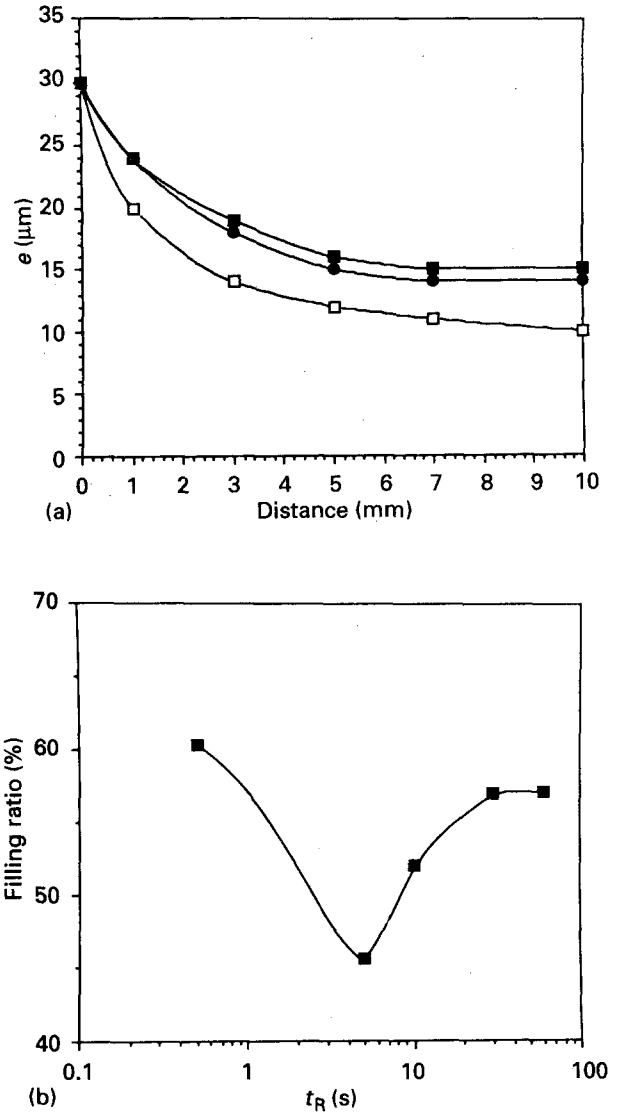

Figure 1 PyC infiltration along the 60 μm model pore for $T = 1050\,°C$ and $P = 1$ kPa: (a) deposit thickness e for $t_R = (\blacksquare)$ 0.5 s, (□) 5 s and (●) 60 s; (b) variations of the filling ratio as a function of t_R.

3. Results

3.1. Thickness profiles and filling ratios

In order to shorten the duration of the experimental study (which consisted of a large number of experiments owing to the number of parameters taken into account), each deposition/infiltration run has been limited to a maximum duration of 200 h. As a result, under the experimental conditions specified in Section 2, it has not been possible to fill totally the two larger pores (which $h = 120$ and 320 μm, respectively). The duration of each run was calculated so that the smaller pore ($h = 60$ μm) was systematically plugged by the PyC deposit at its entrance, at the end of the experiment. For the 120 and 360 μm pores, whose filling was not always complete, a constant deposition rate versus time was assumed, in order to calculate the filling ratio value at pore entrance plugging, by extrapolation.

3.2. Influence of residence time

The thickness profiles, measured along the z-axis of the 60 μm pore after pore entrance blocking, are shown in Fig. 1a for $T = 1050\,°C$, $P = 1$ kPa and three values of the residence time t_R (t_R being the main part of a pulse duration, as explained in Part I [11]). The thickness gradient along the pore is minimized at very low (i.e. $t_R = 0.5$ s) or very large ($t_R = 60$ s) residence time values.

The filling ratios δ_i (with i standing for the size of the pore, i.e. 60, 120 or 320 μm) are derived from the thickness profiles, as stated in Section 2. The variations of δ_{60} as a function of t_R are shown in Fig. 1b. First, the corresponding curve goes through a rather deep minimum for intermediate residence time values (i.e. $t_R = 5$ s) and, second, it shows that the highest filling of the pore is achieved for the lowest values of the gas residence time ($\delta_{60} = 60\%$ for $t_R = 0.5$ s).

The variations of the filling ratios δ_i (with $i = 60$, 120 and 320) as a function of the residence time are shown in Fig. 2, for three different values of the pressure. All the corresponding curves exhibit a minimum and a plateau (for long residence times), which are more or less pronounced depending on the experimental conditions. The value of t_R corresponding to the minimum (see Fig. 2a) seems independent of the pore size but changes slightly as the pressure is increased.

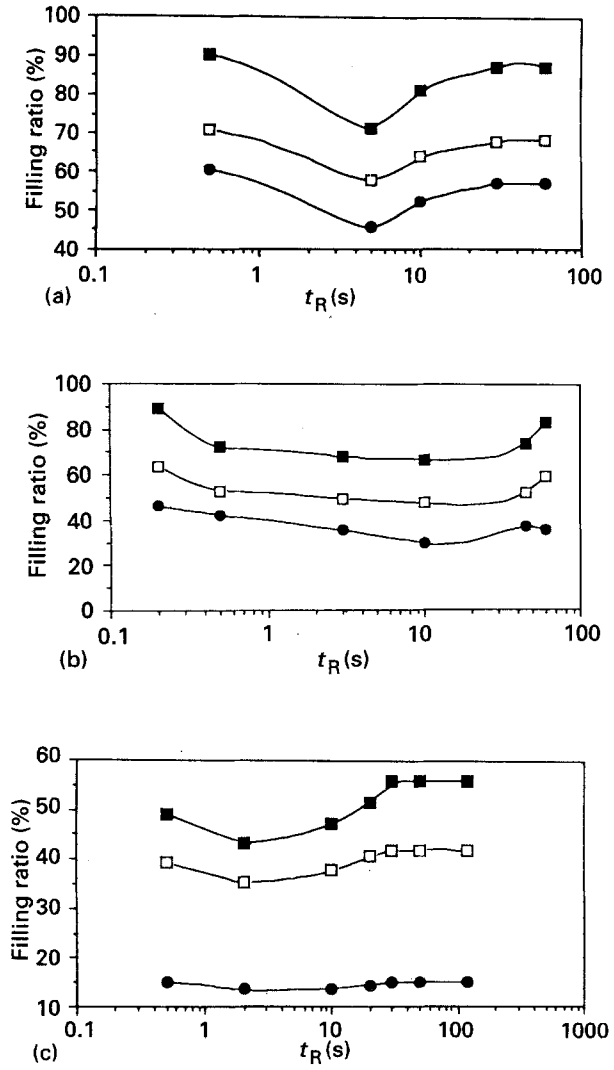

Figure 2 Variations of the filling ratio of the three model pores as a function of residence time for $T = 1050\,°C$ and (a) $P = 1$ kPa, (b) $P = 3$ kPa and (c) $P = 10$ kPa: (●) δ_{60}, (□) δ_{120}, (■) δ_{320}.

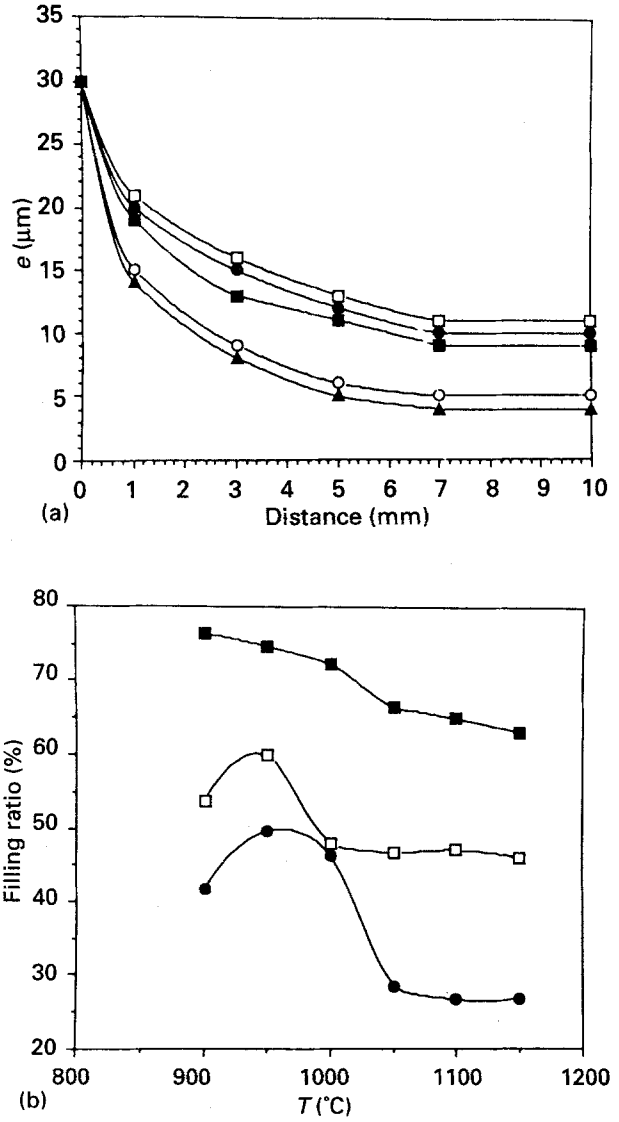

Figure 3 PyC infiltration along the model pores as a function of the temperature for $P = 3$ kPa and $t_R = 10$ s: (a) deposit thickness e at (■) 900 °C, (□) 950 °C, (●) 1000 °C, (○) 1050 °C and (▲) 1150 °C along the 60 μm model pore at pore entrance blocking and (b) filling ratios (●) δ_{60}, (□) δ_{120} and (■) δ_{320} for the three model pores calculated at pore entrance blocking.

3.3. Influence of temperature

The thickness profiles along the 60 μm pore, at pore entrance blocking, are shown in Fig. 3a for different temperature values (with $900 < T < 1150\,°C$) together with the corresponding thermal variations of the filling ratio δ_{60} (Fig. 3b). It appears that the PyC thickness gradient along the pore is reduced for medium temperatures (950–1000 °C).

The thermal variations of the filling ratio δ_i exhibit a maximum with the following features: (i) it is well defined for the small size pores (60 and 120 μm), (ii) it is slightly shifted towards the low temperatures and seems to vanish as the pore size is increased, and (iii) the maximum pore filling decreases (roughly from 80 to 50%) as the pore size decreases from 320 to 60 μm, an already well-known feature for the I-CVI of model pores [1, 2]. Finally, beyond about 1050 °C, the values of the filling ratios do not change any longer as the temperature is raised, whatever the pore size.

In short, this part of the study emphasizes the interest of performing the P-CVI at medium or low temperatures in order to achieve a high degree of pore filling by PyC.

3.4. Influence of pressure

The influence of the propane pressure on the PyC thickness profile along the 60 μm pore axis (at pore entrance blocking) is shown in Fig. 4 for two values of the temperature (950 and 1050 °C) and $t_R = 10$ s. Generally speaking and as already known for I-CVI [1, 2], decreasing the pressure in the infiltration chamber strongly reduces the thickness gradient along the pore (at least under these temperature and residence-time conditions).

The corresponding variations of the filling ratio δ_{60} as a function of the pressure of propane are shown in Fig. 5 on a double logarithmic plot. Within the whole pressure range studied here (extending from pressures as low as 1 kPa to pressures as high as 100 kPa), the curves are observed to be linear. As a result, the variations of δ_{60} as a function of the pressure of propane obey the following equation:

$$\delta_{60},\, T, P \;=\; \delta^0_{60,T,1}\, P_{C_3H_8}^{-0.56}$$

$$\delta^0_{60,T,1} \;=\; \delta_{60,T} \quad \text{for } P \;=\; 1\,\text{kPa} \qquad (1)$$

Thus, decreasing the pressure of propane in the infiltration chamber in the P-CVI of PyC significantly

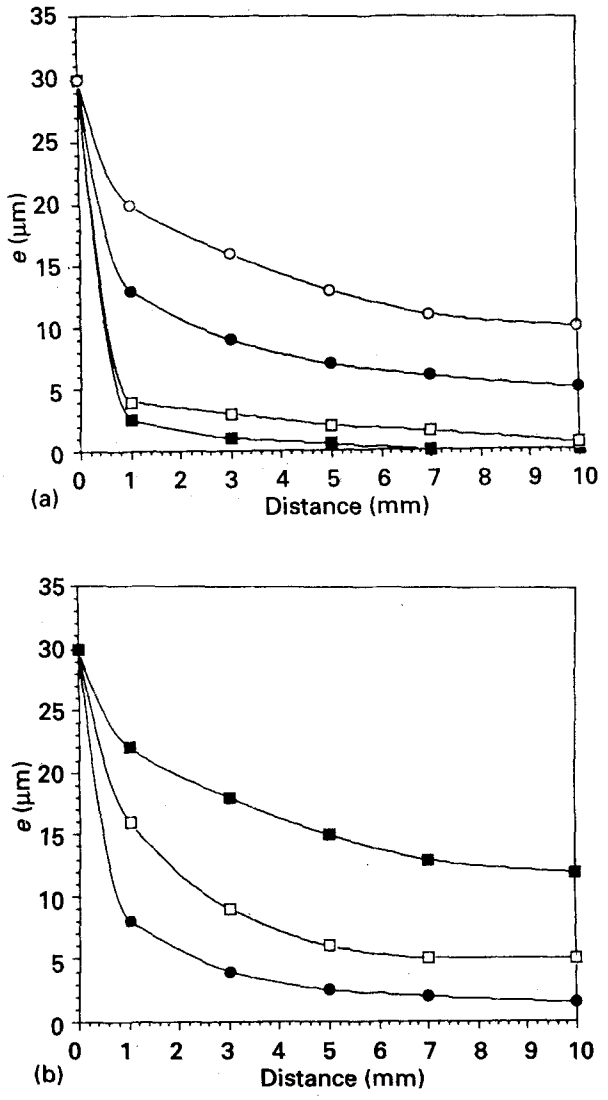

Figure 4 PyC thickness profiles along the 60 μm model pore (at pore entrance blocking) as a function of the total propane pressure and for $t_R = 10$ s: (a) $T = 950\,°C$ and $P = (○)$ 3 kPa, (●) 10 kPa, (□) 50 kPa, (■) 100 kPa; (b) $T = 1050\,°C$ and $P = (■)$ 1 kPa, (□) 3 kPa, (●) 10 kPa.

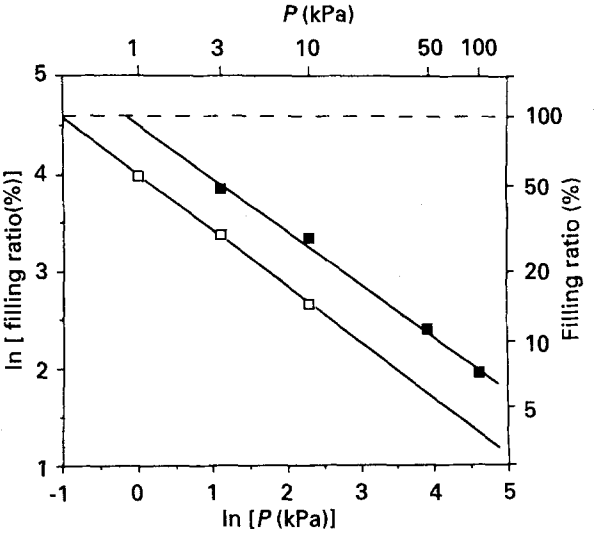

Figure 5 Variations of the filling ratio of the 60 μm model pore (at pore entrance blocking) with the total pressure of propane, shown on a double logarithmic plot (■) 950 °C and (□) 1050 °C with $t_R = 10$ s.

improves the quality of the pore infiltration (as already reported for I-CVI), very low pressures (1 kPa or less) being apparently necessary to achieve an almost complete filling of pores of this size.

3.5. Influence of the nature of the gas precursor

The influence of the nature of the source species (propane or methane) on the thickness profile (at pore entrance blocking) is shown in Fig. 6 for the 60 μm pore, $T = 1050\,°C$, $t_R = 10$ s and two pressure values. Under such conditions, the quality of the infiltration is better with methane whatever the pressure of the hydrocarbon in the infiltration chamber. The improvement in the PyC thickness profile along the pore, observed when propane is replaced by methane, is more pronounced at low pressures (e.g. 3 kPa) than at high pressures (10 kPa).

Furthermore, the δ_{60} ratio observed for methane is much higher than for propane, their relative values remaining almost unchanged as the pressure is

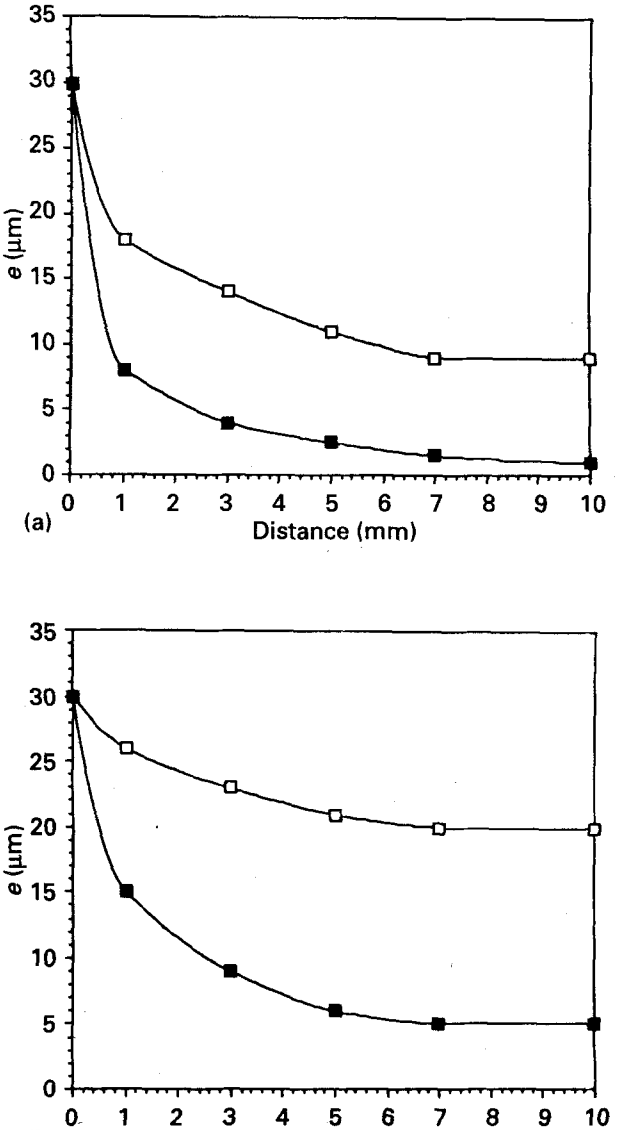

Figure 6 Variations of PyC deposit thickness e along the 60 μm model pore (at pore entrance blocking) for (■) propane and (□) methane gas precursor with $T = 1050\,°C$ and $t_R = 10$ s: (a) $P = 10$ kPa, (b) $P = 3$ kPa.

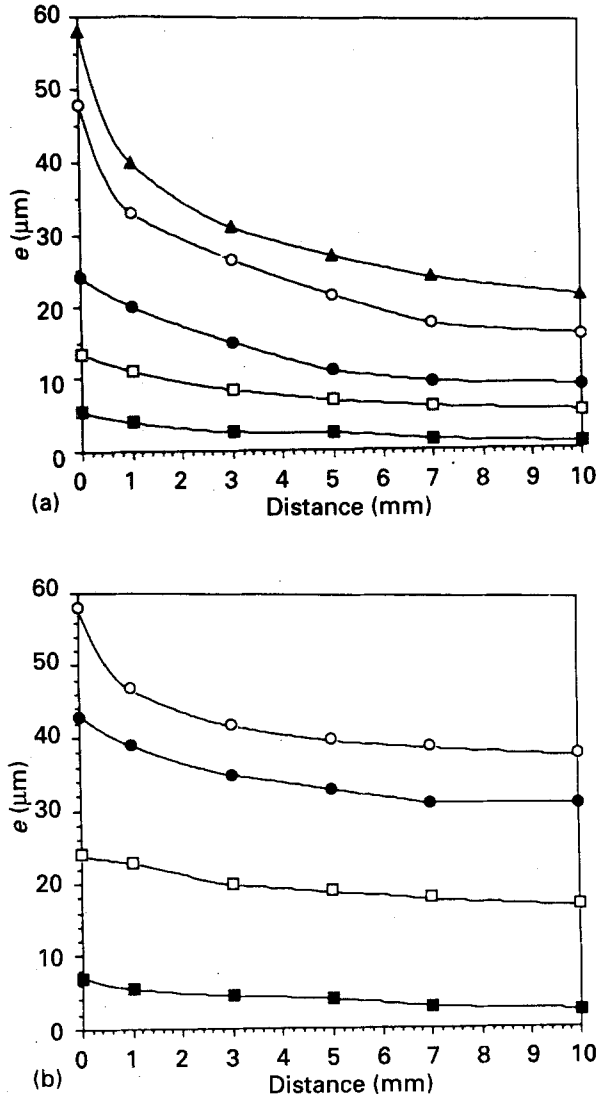

Figure 7 Variation of PyC deposit thickness e along the 120 μm model pore as a function of infiltration total duration. (a) P-CVI, $T = 1150\,°C$, $P = 3$ kPa, $t_R = 10$ s and total duration (■) 3 h, (□) 6 h, (●) 10 h, (○) 18 h, (▲) 22 h. (b) I-CVI, $T = 1050\,°C$, $P = 3$ kPa, $Q = 60$ sccm and total duration (■) 10 h, (□) 30 h, (●) 53 h, (○) 72 h.

lowered: $\delta_{60}(CH_4)/\delta_{60}(C_3H_8) = 2.9$ for $P = 10$ kPa and $\delta_{60}(CH_4)/\delta_{60}(C_3H_8) = 2.6$ for $P = 3$ kPa.

3.6. Influence of infiltration duration

The influence of the infiltration duration (calculated as the product of the pulse duration and the number of pulses) on the PyC thickness profile along the 120 μm pore is shown in Fig. 7 together with that (for the purpose of comparison) corresponding to I-CVI, both performed under similar experimental conditions in the same hot-wall apparatus.

For P-CVI, the data show that the thickness of the PyC deposit at a given z-value along the pore varies in a linear manner as a function of the infiltration duration. As a consequence, the variations of the related δ_{120} filling ratio as a function of time obey a similar linear law, as shown in Fig. 8. This is no longer the case for I-CVI, at least for experimental conditions which have been used in the present work. It appears from a comparison of the curves that (i) the infiltration rate is higher for P-CVI than for I-CVI (the blocking

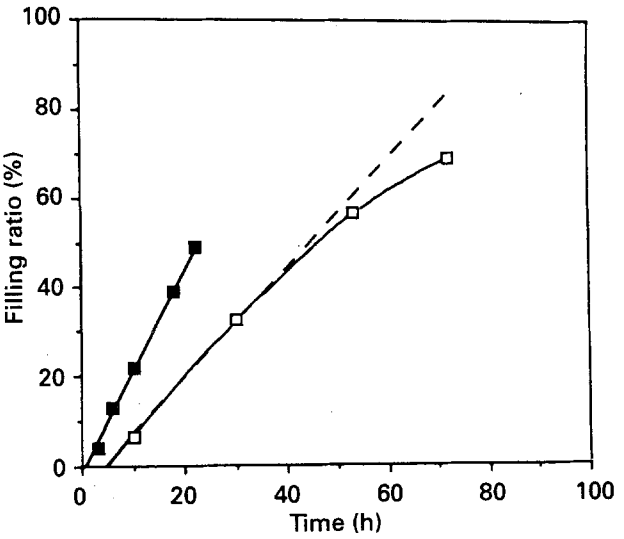

Figure 8 Variation of the filling ratio of the 120 μm model pore as a function of infiltration duration: (■) P-CVI, $T = 1150\,°C$, $P = 3$ kPa, $t_R = 10$ s and (□) I-CVI, $T = 1050\,°C$, $P = 3$ kPa, $Q = 60$ sccm.

of the pore being achieved for $t = 22$ h for the former and only for $t = 72$ h for the latter), and (ii) the filling ratio at pore blocking is higher for I-CVI. One could argue that these differences could be due to the fact that the experiments have been performed at different temperatures (1150 °C for P-CVI and 1050 °C for I-CVI). However, the PyC thickness profiles shown in Fig. 3a suggest that the influence of temperature is weak within the 1050–1150 °C range.

3.7. Anisotropy of PyC deposit along the pore

The extinction angle Ae (measured in polarized light with an optical microscope) is known to characterize the PyC anisotropy. Its value increases from 4° (isotropic PyC) to 20° (rough laminar PyC) as the anisotropy of the PyC deposit increases. Its variations along the longitudinal axis of the 60 μm model pore are shown in Table I for different values of the residence time t_R of the propane precursor in the deposition chamber.

Short residence times (i.e. $t_R = 0.2$ s) yield a PyC deposit whose anisotropy is relatively low ($Ae = 12°$, corresponding to dark/smooth laminar) and homogeneous along the pore axis. Conversely, when t_R is raised (from 0.2 to 60 s), the PyC microstructure exhibits the following features: (i) the PyC anisotropy is very high ($Ae = 20°$; rough laminar) at the substrate surface ($z = 0$) and near the pore entrance ($z \leqslant 1$ or

TABLE I Variations of extinction angle Ae (deg) along the longitudinal 60 μm pore axis ($T = 1050\,°C$, $P = 3$ kPa)

Residence time, t_R (s)	Location along the pore axis, z(mm)				
	0	1	3	5	10
0.2	12	12	12	12	12
0.5	20	20	15	12	12
10	20	20	19	15.5	14.5
60	20	20	17	13	12

2 mm) and (ii) an anisotropy gradient is observed along the pore which is steep for low ($t_R = 0.5$ s) or high ($t_R = 60$ s) residence times and less pronounced for intermediate values ($t_R = 10$ s).

There is thus a clear correlation between the anisotropy of the PyC deposited at the substrate external surface and along the model pores, on the one hand, and the duration of the pulse, on the other hand, which will be discussed in the next section.

4. Discussion

The data which have been presented in Section 3 show that the total pressure P and the temperature T are two important parameters for controlling the kinetics of the infiltration process in P-CVI, as already well established for the related I-CVI [1, 2]. However, P-CVI provides an additional controlling parameter, the residence time t_R, which appears particularly important when the gas phase undergoes chemical change as it is maintained at high temperatures in a closed reactor vessel (which is actually the case for a hydrocarbon precursor such as propane). For the purpose of the discussion, a pulse can be divided into two main stages:

(i) At the beginning of the pulse, a short stage (stage 1), whose duration is typically of the order of a few hundredths of a second, during which the C_3H_8 gas precursor is forced to penetrate the pore (the mass transfer of the gaseous reactant being by forced convection).

(ii) In a second stage, which corresponds to the majority of the pulse (i.e. a few tenths of a second to a few seconds and even several tens of seconds) the gas phase, entrapped in the closed infiltration chamber and maintained at a high temperature, undergoes a continuous change in chemical composition. During this stage, referred to as stage 2 or "gas phase maturation", dehydrogenation, condensation and cyclization phenomena occur giving rise to the formation of aromatic and large-size molecules [13]. During stage 2, two deposit processes are in competition [9]: process I which is characterized by heterogeneous reactions involving molecules akin to propane, i.e. of rather small sizes and highly hydrogenated, and process II which takes place when the gas phase maturation is better achieved and corresponds to the direct condensation of the large aromatic species on to the substrate surface. Since in P-CVI the filling–holding–evacuating sequence is repeated periodically, the corresponding PyC deposit is itself a sequence of several elemental deposits formed according to processes I or II, depending on the value of t_R.

4.1. Influence of residence time on thickness profile

The residence time t_R has a great influence on the PyC thickness profile along the model pores and on the related filling ratio (δ_i), as shown in Figs 1 and 2. In P-CVI, the interesting t_R values, i.e. those yielding high filling ratios, are either the low t_R values (corresponding mainly to filling of the pore by forced convection (stage 1) with very limited gas phase maturation and being higher as the pore size is lower), or the high t_R values (corresponding mainly to stage 2 and limited by both gas-phase depletion and the inhibiting effect of the increase of hydrogen partial pressure in the pore).

The effect of t_R on the PyC thickness profile along the pore axis (e.g. the 60 μm pore), under given T–P conditions (e.g. $T = 1050\,°C$ and $P = 3$ kPa) can be discussed on the basis of the two deposition processes (process I and process II) by considering the PyC thickness per pulse, $e_{p,z,t_R^{(i)}}$ and $e_{p,z,t_R^{(j)}}$, deposited at a given z abscissa during two pulses of different durations $t_R^{(i)}$ and $t_R^{(j)}$, with $t_R^{(i)} > t_R^{(j)}$, as shown in Fig. 9. The differential thickness per pulse, $\Delta e_{p,z}$, defined according to the equation

$$\Delta e_{p,z} = e_{p,z,t_R^{(i)}} - e_{p,z,t_R^{(j)}} \qquad (2)$$

is assumed to represent that portion of the PyC deposited during a pulse corresponding to a given mean degree of gas phase maturation (defined between the two limits $t_R^{(j)}$ and $t_R^{(i)}$). In other words, $\Delta e_{p,z}$ allows one to subtract the PyC thickness deposited at the beginning of a pulse from the overall PyC thickness per pulse and to consider only that related to a mean degree of gas phase maturation.

Equation 2 can be rewritten, considering the deposit occurring at the pore entrance, i.e. at $z = 0$, as

$$\Delta e_{p,0} = \Delta e_{p,0,t_R^{(i)}} - \Delta e_{p,0,t_R^{(j)}} \qquad (2')$$

The number of pulses n which would be necessary for achieving pore blocking at $z = 0$ by this specific PyC

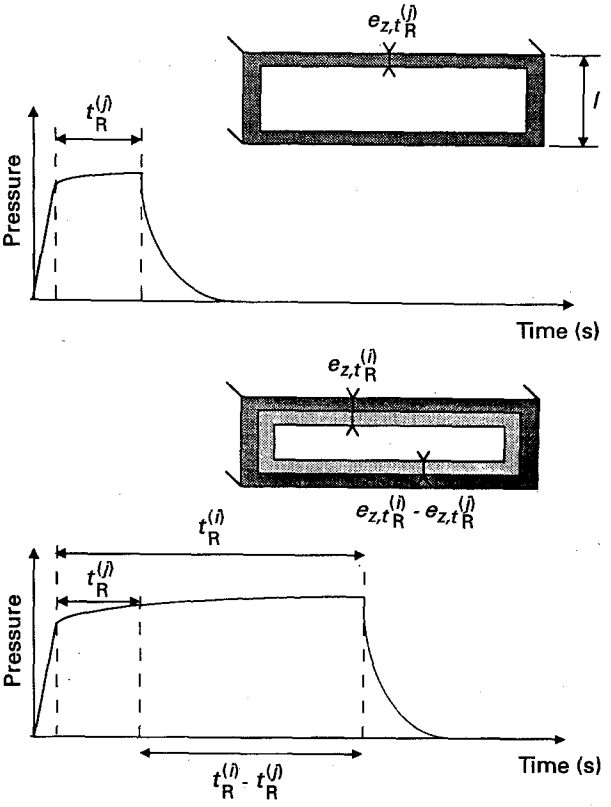

Figure 9 PyC thickness $e_{z,t_R^{(i)}}$, $e_{z,t_R^{(j)}}$ and $e_{z,t_R^{(i)}} - e_{z,t_R^{(j)}}$ deposited in a pore cross-section at a given abscissa z, during pulses of different durations corresponding to different degree of gas phase maturation (schematic).

deposited under such a controlled condition of gas phase maturation is defined by

$$n = \frac{h/2}{\Delta e_{p,0}} \quad (3)$$

Knowing this value of n it is thus possible to calculate, for each value of z, the PyC thickness deposited under the condition of gas phase maturation defined above, at pore entrance blocking:

$$e_z^v = \Delta e_{p,z} n \quad (4)$$

Equation 4 can be rewritten as

$$e_z^v = \frac{\Delta e_{p,z}}{\Delta e_{p,0}}\left(\frac{h}{2}\right) \quad (4')$$

The values of the PyC thickness deposited per pulse, $e_{p,z}$, are directly calculated from the experimental curves $e = f(z)$ (see for example Fig. 1a). Their variations as a function of z are shown in Fig. 10 for the 60 μm model pore, $T = 1050\,°C$, $P = 3$ kPa and t_R ranging from 0.2 to 60 s. Introducing these values in Equations 2, 2′ and 4′ allows one to draw virtual thickness profiles, $e_z^v = f(z)$, that would correspond to PyC deposited along the pore axis under the $t_R^{(i)}$–$t_R^{(j)}$ gas phase maturation conditions, at pore entrance blocking (Table I). These profiles are shown in Fig. 11 for the 60 μm pore and will be used to discuss the effect of t_R.

4.1.1. Very low t_R values ($t_R < 0.05$ s)

When the pulse is of very short duration, the majority of the pulse corresponds to the filling of the pore by the C_3H_8 precursor (stage 1) which occurs by forced convection with almost no maturation of the gas phase. Under such conditions, the thickness profile along the pore should be flat (if the pulse duration, i.e. t_R to a first approximation, is sufficient to allow precursor transport to the pore centre). Such a condition is fulfilled, for $t_R < 0.05$ s, when the pore size is large enough (e.g. for $h = 320$ μm, as will be established later) but it may be no longer the case for pores of very small sizes, as established by Sotirchos [9] for the infiltration of < 1 μm pores by SiC deposited from a CH_3SiCl_3–H_2 mixture. This stage 1 corresponds to the real P-CVI, as described by Sugiyama and Ohzawa [8], where the reactant mass transfer along the pore occurs mainly by forced convection (i.e. almost without diffusion). However, such very short residence time values are too low to be accessible with our apparatus (and *a fortiori* with a large industrial furnace).

The theoretical PyC thickness deposited per pulse, e_{pp}, under such conditions of very short t_R can be calculated from the amount of propane entrapped in the rectangular cross-section model pore, assuming that each C_3H_8 molecule is cracked into carbon during t_R. The calculations lead to the following simple equation (see Equations A4 and A5 in the Appendix):

$$e_{pp} = Kh$$

where K is a dimensionless constant given by

$$K = \frac{1}{2240}\left(\frac{P}{P_0}\right)\frac{T_0}{T}$$

equal to 2.81×10^{-6} for $P = 3$ kPa and $T = 1050\,°C$. For the three model pores considered here with $h = 60$, 120 and 320 μm, the corresponding e_{pp} values are 0.168, 0.337 and 0.899 nm, respectively. These values are undoubtedly overestimated since all the propane is not actually consumed. However, they can be used to estimate the values of t_R necessary to achieve a flat PyC thickness profile along the pore axis. With a deposition rate of 3 nm s^{-1} (derived from the $e_{p,0}$ value, 0.6 nm/pulse, corresponding to the lowest t_R value of 0.2 s in Table II), a PyC thickness equal to e_{pp} will be achieved in 56, 112 and 300 ms for $h = 60$, 120 and 320 μm, respectively. These results show that flat profiles along the pore axis could be expected only for the 320 μm pore, taking into account the limitation of our apparatus ($t_R \geqslant 0.2$ s).

Since under the condition of pore filling by forced-convection mass transfer (i.e. very low t_R values) the PyC thickness profile along the pore is assumed to be

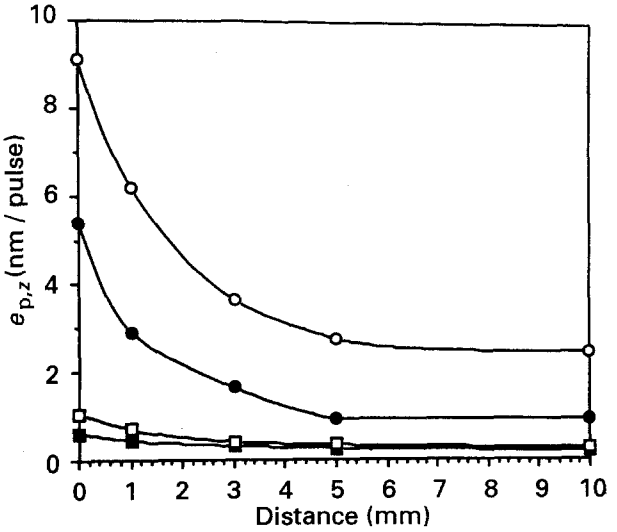

Figure 10 Variation of $e_{p,z}$ with distance z along the 60 μm model pore for $T = 1050\,°C$ and $P = 3$ kPa; t_R = (■) 0.2 s, (□) 0.5 s, (●) 10 s, (○) 60 s.

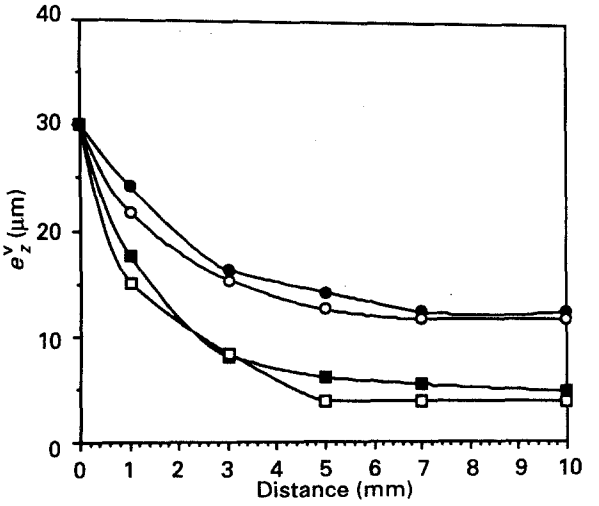

Figure 11 Variations of e_z^v with distance z along the 60 μm model pore for $T = 1050\,°C$ and $P = 3$ kPa; $t_R^{(i)}$ and $t_R^{(j)}$ = (○) 0.2 and 0 s, (■) 0.5 and 0.2 s, (□) 10 and 0.5 s, (●) 60 and 10 s, respectively.

TABLE II Variations of the differential PyC thickness per pulse, $\Delta e_{p,z}$ (nm/pulse) along the longitudinal 60 μm pore axis for different residence times t_R ($T = 1050\,°C$, $P = 3$ kPa)

$t_R^{(j)}$ (s)	$t_R^{(i)}$ (s)	Location along the pore axis, z(mm)				
		0	1	3	5	10
0	0.2	0.60	0.45	0.33	0.26	0.21
0.2	0.5	0.44	0.26	0.09	0.10	0.07
0.5	10	4.30	2.20	1.20	0.56	0.63
10	60	3.70	3.30	2.10	1.83	1.52

flat, the pore filling ratio δ_i corresponding to a given number of pulses n can be written (see Equation A6 of the Appendix) as

$$\delta_i = 1 - (1 - 2K)^n$$

with δ_i no longer depending on the pore size. Under such conditions, the infiltration of the model pore is expected to be very good (flat PyC thickness profile) but a large number of pulses is necessary to achieve a high filling ratio. As an example, a δ_i value of 94% will require $n = 500\,000$ pulses for $T = 1050\,°C$ and $P = 3$ kPa. It is worthy of note that a δ_{320} value of the order of 90% has been observed for $t_R = 0.2$ s, $T = 1050\,°C$ and $P = 3$ kPa (Fig. 2b) suggesting that the infiltration may have proceeded mainly according to this mode (stage 1) for these specific conditions (low t_R value and pore of large size).

4.1.2. Low t_R values ($0.05 < t_R < 0.2$ s)

Within the range $0.05 < t_R < 0.2$, the infiltration of the model pores involves now the two stages (stage 1 and stage 2) and the PyC thickness profile is no longer expected to be flat. In other words, a PyC thickness gradient is present along the pore, as already reported for the related I-CVI process [1, 2, 14]. This feature is clearly apparent from both the experimental curves (Figs 1a and 10) and the calculated virtual thickness profile (Fig. 11).

For these t_R values, the gas phase composition in the dead volume (i.e. that corresponding to the closed reaction vessel) is only slightly changed during the pulse, since the amount of PyC deposited is low. As an example, the PyC thickness deposited on the external substrate surface ($z = 0$) during a pulse of 0.2 s is only 7% of that corresponding to a 60 s pulse (Fig. 10). The PyC deposition occurring during such short pulses is thought to result from the surface adsorption and reaction of small and highly hydrogenated species akin to propane, i.e. mainly according to process I with little gas phase maturation. These molecules diffuse easily along the pores and the filling ratios are very good (Fig. 1b), whatever the pore size, with a PyC thickness gradient along the pore that is not too steep.

4.1.3. Intermediate t_R values ($0.2 < t_R < 10$ s)

The e_z^v profiles calculated for significant degrees of gas phase maturation, i.e. between $t_R^{(i)} = 0.5$ s and $t_R^{(j)} = 0.2$ s or between $t_R^{(i)} = 10$ s and $t_R^{(j)} = 0.5$ s, as shown in Fig. 11, exhibit strong gradients along the pore axis. It is thought that the PyC deposited on the external substrate surface and in the pore near its entrance grows according to process II. As a matter of fact, the large molecules formed in the gas phase (such as pyrene and phenanthrene) as the result of dehydrogenation–cyclization–condensation processes and which have been actually detected experimentally [11] have indeed a high probability of stacking near the pore entrance and their diffusion along the pore is limited (particularly when the pore size is limited, e.g. for the 60 μm-pore). As a consequence, at $z = 10$ mm (pore centre) the PyC is thought to grow mainly according to process I, i.e. as a result of the cracking of small and hydrogenated molecules (whose lifetime and mobility are higher). The PyC thickness at the pore centre is much lower owing to gas phase depletion and the inhibiting effect of hydrogen. These intermediate t_R values correspond to the worst conditions, in terms of thickness gradient and pore filling ratio (Figs 1b and 11).

4.1.4. High t_R values ($t_R > 10$ s)

The e_z^v thickness profile calculated for $t_R^{(i)} = 60$ s and $t_R^{(j)} = 10$ s (Fig. 11) exhibits a less pronounced gradient. This might be due to a strong decrease of the amount of the large aromatic molecules because of gas phase depletion and/or the increase of hydrogen concentration. As a result, the species present in the gas phase (for these high degrees of maturation) might be again smaller and more hydrogenated. This assumption is also supported by the methane concentration (methane leads to weak gradients in P-CVI and even to inverse gradients in I-CVI [15]) which has been reported to be high for long pulses. These smaller molecules diffuse well along the pore, as previously mentioned. The PyC growth occurs according to a process which is not yet fully elucidated but which could be a mixed process.

4.2. Correlation between residence time and PyC anisotropy

For short residence times, e.g. $t_R = 0.2$ s, the extinction angle is low ($Ae = 12°$) whatever the value of the abscissa z along the pore axis (Table 1). As discussed in Section 4.1, the chemical species which lead to PyC are small and highly hydrogenated. As a consequence, their diffusion in the pore is easy (with the result that the thickness gradient along the pore is not too steep, see Table II and Fig. 11) but the PyC is poorly organized (Table 1).

For intermediate residence times (e.g. $t_R = 0.5$ or 10 s) both an Ae gradient (Table 1) and a thickness gradient (Table II and Fig. 11) are present along the model pore. Gas phase maturation (which is significant for these values of t_R) leads to the formation of large and dehydrogenated (aromatic) molecules, as already discussed, which tend to preferentially stack on the pore wall near the pore entrance (i.e. at about $0 < z < 1$ mm). The improvement of Ae (and thus of the PyC anisotropy) observed near the pore entrance

($Ae = 20°$) is thought to result from the direct condensation of these molecules on to the wall and the external surface of the substrate. The higher the PyC thickness deposited according to process II (with respect to that formed according to process I), the higher is the Ae gradient along the pore (Table 1). As an example, at $z = 10$ mm (pore centre) we have

$$\Delta e_p = 0.21 \text{ nm and } Ae = 12°$$
$$\text{for } t_R^{(i)} = 0.2, \quad t_R^{(j)} = 0 \text{ s}$$
$$\Delta e_p = 0.07 \text{ nm and } Ae = 12°$$
$$\text{for } t_R^{(i)} = 0.5, \quad t_R^{(j)} = 0.2 \text{ s}$$

(process I only)

$$\Delta e_p = 0.63 \text{ nm and } Ae = 14.5°$$
$$\text{for } t_R^{(i)} = 10, \quad t_R^{(j)} = 0.5 \text{ s}$$

(processes I and II)

For high residence times (e.g. $t_R = 60$ s) the gas phase maturation is almost fully achieved. The concentration of the large aromatic species is much lower and the formation of both methane and hydrogen enhanced. As a result, the PyC rate of deposition decreases and tends to zero (inhibition by hydrogen). At the substrate external surface ($z = 0$) Ae is still very high (20°) but in the middle of the pore ($z = 10$ mm) Ae decreases (12°) because the PyC thickness deposited during the last part of the pulse is poorly organized and important with respect to the overall PyC thickness at this location ($e_{p,10,0.2-10} = 0.7$ nm and $e_{p,10,10-60} = 1.52$ nm).

There is thus a rather clear correlation between the PyC anisotropy, on the one hand, and the residence time, on the other hand. More details about the anisotropy of the PyC deposited are given elsewhere [12].

4.3. Influence of both temperature and pressure on the thickness profile

Both temperature and pressure have a strong influence on the PyC thickness profile along the model pores in P-CVI, at least for the t_R range studied in the present work, as previously reported for I-CVI [1, 2, 14]. Generally speaking, decreasing T and P favours in-depth deposition (Figs 3a and 4).

The variations of the filling ratio δ_i as a function of temperature are more important as the pore is smaller (Fig. 3b). At $t_R = 10$ s, process II mainly controls the deposit particularly when temperature is high (the gas phase maturation being faster). Under such conditions, a fast blocking of the pore entrance occurs because of condensation of the large (aromatic) molecules, with the result that the filling ratio is low, particularly for the smaller pores ($\delta_{60} = 25\%$ and $\delta_{120} = 45\%$ for $T = 1100$ °C). Finally, the filling ratio decreases from an optimum value which is achieved at about 950 °C as the temperature is lowered. This feature, which is observed only for the 60 and 120 μm pores, is still incompletely understood and might be related to soot formation (which has been actually observed experimentally).

An increase of the pressure at $950 < T < 1050$ °C and $t_R = 10$ s (conditions corresponding to a significant degree of gas phase maturation) is thought to lead to a rapid control of the PyC deposition by process II and is thus unfavourable to in-depth infiltration (Fig. 4).

4.4. Influence of precursor nature on the thickness profile

The nature of the precursor (and thus its thermal stability and ability to yield carbon) is another parameter which has a great influence on the PyC thickness profiles along the model pores (Fig. 6). As an example, when propane is replaced by methane the filling ratio is raised from 28 to 74% for the 60 μm pore under the same experimental conditions ($T = 1050$ °C, $P = 3$ kPa and $t_R = 10$ s). As the thermal stability of methane is higher, its maturation is slower than that of propane for a given t_R value and thus the in-depth diffusion of the source species (as small molecules) is favoured, resulting in a higher filling of the pore by the PyC deposit (process I). In other words, the deposition process (mainly process I) of PyC from CH_4 for $t_R = 10$ s might be close to that for C_3H_8 at $t_R = 0.2$ s, the same degree of gas phase maturation being achieved at different residence times.

Another important feature is that the PyC deposition rate per pulse is one order of magnitude higher with C_3H_8 than with CH_4 under the same deposition conditions, which does not favour in-depth infiltration. However, if the experimental conditions are chosen differently in order to yield the same deposition rate per pulse, propane appears to be a better source than methane for infiltration [11].

4.5. Influence of total infiltration duration on the thickness profile

The P-CVI experiments performed with the 120 μm model pore (Fig. 7a) show that, surprisingly, the PyC deposition rate remains almost constant as infiltration proceeds, i.e. as the pore size decreases with time. As a result, the thickness of the PyC deposited at a given z value, $e_z(t)$, is proportional to the number of pulses and can be expressed as

$$e_z(t) = e_{p,z}(n - n_0) \qquad (5)$$

where n_0 is the initial number of pulses which are necessary to fill the porosity/rugosity of the pore wall and to measure a deposit. The reason why the PyC deposition rate remains constant in P-CVI is not yet known.

5. Conclusions

The experimental data reported in Section 3 and the discussion presented in Section 4 lead to the following main conclusions:

(i) Model straight pores with rectangular cross-sections and sizes ranging from 60 to 320 μm have been infiltrated with pyrocarbon deposited from CH_4 and C_3H_8 precursors under P-CVI conditions.

(ii) The main experimental parameters controlling the quality of the infiltration are temperature and pressure, as previously reported for I-CVI, but also the residence time which appears as a key parameter in P-CVI (inasmuch as it controls both the filling ratio and the anisotropy of the PyC deposit).

(iii) There are two important steps during a pulse. At the beginning of the pulse (stage 1), a mass transfer of the source species occurs by forced convection along the pore during a few hundredths or tenths of a second (depending on the pore size). Then during the majority of the pulse (stage 2), the hydrocarbon gas phase undergoes a key maturation phenomenon.

(iv) During stage 2 the PyC deposition occurs ac cording to two successive or simultaneous process mechanisms. In process I, PyC is formed from small, highly hydrogenated molecules, whereas in process II it is formed by simple condensation on the pore wall of large aromatic intermediate species. The former is favourable to in-depth infiltration and yields a PyC deposit with a low anisotropy, whereas the latter takes place preferentially near the pore entrance and results in a highly anisotropic PyC. The respective contribution of the two processes are highly dependent on the residence time t_R (which controls the degree of gas phase maturation at given T, P) and there is a direct correlation between t_R, on the one hand, and thickness gradient of PyC as well as anisotropy along the pore, on the other hand.

(v) Very short pulses might yield flat PyC thickness profiles along the pore. Unfortunately, such conditions could not be achieved in the present work due to experimental limitation (as would be also the case for large furnaces at the plant level).

(vi) Short residence times (e.g. $t_R \simeq 0.5$ s) associated with low propane pressures (e.g. a few kPa) and temperature ranging from 900 to 1000 °C yield filling ratios equivalent to and even higher than those reported for I-CVI with the restriction that, under such conditions, a large number of pulses is necessary.

(vii) Replacing propane by methane results, under the same experimental conditions, in better infiltrations owing to the higher thermal stability of CH_4 which limits the gas phase maturation (i.e. the formation of large aromatic molecules).

(viii) Although P-CVI may appear to exhibit a limited interest with respect to I-CVI (its advantages being mitigated by its constraints at the industrial level), it offers an efficient way for controlling the microstructure of the solid which is deposited.

Acknowledgements

This work has been supported by SEP through a grant given to P.D. The authors are indebted to S. Goujard and C. Robin-Brosse from SEP for technical assistance and valuable discussions.

Appendix

The potential PyC thickness deposited per pulse, e_{pp}, related to the force convection step (stage 1) is defined as the thickness of PyC that would be formed on the wall of an elementary section of the model pore, located at an abscissa z, from the C_3H_8 molecules present in this section, assuming that the C_3H_8–C conversion is total.

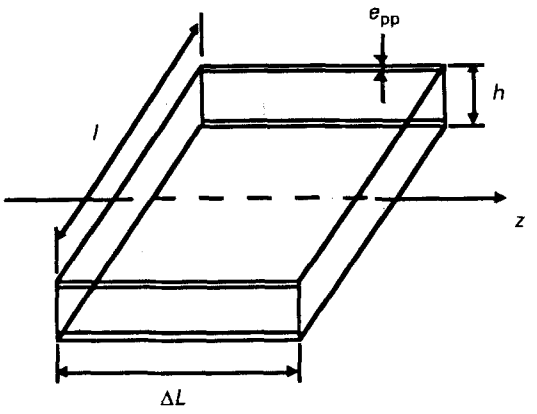

Figure A1 Volume element of a model pore.

Let us consider an elementary pore cross-section of thickness ΔL. It contains at T, P a C_3H_8 volume $\Delta V = lh\Delta L$ (Fig. A1) and the area of the pore cross-section wall is $\Delta S \simeq 2\Delta Ll$ neglecting $2hl$ (since h is assumed to be negligible with respect to ΔL). Assuming that propane obeys the perfect gas law, the number of moles of C_3H_8 entrapped in the elementary volume under the standard T, P conditions is

$$\eta = (lh\Delta L)\frac{P}{P_0}\left(\frac{T_0}{T}\right)\frac{1}{22400} \qquad \text{(A1)}$$

l, h and ΔL being expressed in cm. Assuming that one mole of C_3H_8 gives 36 g of carbon and the density of PyC is 1.8 g cm^{-3}, the volume of carbon that could be formed is

$$v_C^{th} = \frac{36}{1.8}\eta = 20\eta \qquad \text{(A2)}$$

and e_{pp} is expressed as

$$e_{pp} = \frac{20\eta}{2\Delta Ll} \qquad \text{(A3)}$$

or

$$e_{pp} = Kh \qquad \text{(A4)}$$

with

$$K = \frac{1}{2240}\left(\frac{P}{P_0}\right)\frac{T_0}{T} \qquad \text{(A5)}$$

For $P = 3$ kPa and $T = 1050 + 273 = 1323$ K, the value of K is 2.81×10^{-6}.

Under the condition of pore filling by forced convection mass transfer, i.e. for very low t_R values, the PyC thickness profile along the pore z axis is expected to be flat. Thus, the pore filling ratio δ_i corresponding to a given number of pulses n can be calculated by considering the cumulative thickness of PyC deposited on to the pore wall. During the first pulse ($n = 1$), the size of the pore decreases from h to

$$h - 2e_{pp} = h - 2Kh = h(1 - 2K)$$

and during the second pulse, from $h(1 - 2K)$ to

$$\begin{aligned} h(1 - 2K) - 2e_{pp} &= h(1 - 2K) - 2h(1 - 2K)K \\ &= h(1 - 2K)(1 - 2K) \\ &= h(1 - 2K)^2 \end{aligned}$$

thus, after n pulses, the size of the pore is $h(1 - 2K)^n$ and the cumulative thickness of PyC is

$$h - h(1 - 2K)^n = h[1 - (1 - 2K)^n]$$

Finally, the pore filling ratio is

$$\delta_i = \frac{h[1 - (1 - (2K)^n]}{h}$$

or

$$\delta_i = 1 - (1 - 2K)^n \qquad \text{(A6)}$$

References

1. R. NASLAIN and F. LANGLAIS, in "Tailoring Multiphase and Composite Ceramics", edited by R. E. Tressler, G. L. Messing, C. G. Pantano and R. E. Newnham, Materials Science Research Vol. 20 (Plenum, New York, 1986) p. 145.
2. R. NASLAIN, in "Ceramic Matrix Composites", edited by R. Warren (Blackie, Glasgow, 1992) p. 199.
3. W. J. LACKEY and T. L. STARR, in "Fiber Reinforced Ceramic Composites", edited by K. S. Mazdiyasni (Noyes, Park Ridge, New Jersey, 1990) p. 397.
4. S. MIDDLEMAN, *J. Mater. Res.* **4** (1989) 1515.
5. Y. S. LIN, in Proceeding of 11th International Conference on CVD, Seattle, Oct. 1990, edited by K. E. Spear and G. W. Cullen (Electrochemical Society, Pennington, 1990) p. 532.
6. T. M. BESMANN, R. A. LOWDEN, D. P. STINTON and L. L. STARR, Suppl. 5, *J. physique*, Colloque C5, Suppl. 5, **50** (1989) 229.
7. K. SUGIYAMA and T. NAKAMURA, *J. Mater. Sci. Lett.* **6** (1987) 331.
8. K. SUGIYAMA and Y. OHZAWA, *J. Mater. Sci.* **25** (1990) 4511.
9. S. V. SOTIRCHOS, *AIChE Jnl.* **37** (1991) 1365.
10. S. V. SOTIRCHOS and M. TOMADAKIS, in "Chemical Vapor Deposition of Refractory Metals and Ceramics", edited by T. M. Besmann and B. M. Gallois (MRS, Pittsburgh, 1990) p. 73
11. P. DUPEL, R. PAILLER and F. LANGLAIS, *J. Mater. Sci.* **28** (1993) 000.
12. P. DUPEL, X. BOURRAT and R. PAILLER, *Carbon* accepted.
13. C. J. CHEN and M. H. BACK, *ibid.* **17** (1979) 175.
14. P. DUPEL, R. PAILLER, F. LANGLAIS, R. NASLAIN and A. COSTECALDE, *ibid.* accepted.
15. P. LAJZEROWICZ, Thèse doct-ing (numéro d'ordre 606), INPG, Grenoble (1987).

Received 25 June
and accepted 24 August 1993